An evaluation of the relationship between two- and three-dimensional packing in self-organised monolayers and bulk crystals of amphiphilic 2,2′:6′,2″-terpyridines†

Edwin C. Constable,*[a] H.-J. Güntherodt,[b] Catherine E. Housecroft,[a] Leo Merz,‡[ab] Markus Neuburger,[a] Silvia Schaffner[a] and Yaqiu Tao[a]

Received (in Montpellier, France) 8th June 2006, Accepted 13th July 2006
First published as an Advance Article on the web 23rd August 2006
DOI: 10.1039/b608136c

2,2′:6′,2″-Terpyridine (tpy) ligands with pendant octadecyloxy, 4-octyloxyphenyl or 4-octadecyloxyphenyl substituents at the 4′-position have been prepared and structurally characterised. Monolayers of the compounds have been prepared on highly oriented pyrolytic graphite (HOPG) and investigated by STM. The monolayer structure corresponds to the bulk crystal structure if the latter contains planar sheets. The tpy ligands are prochiral and form homochiral domains within the monolayer, providing a spectacular visual representation of the symmetry-breaking concomitant with the formation of a monolayer.

Introduction

The self-organization of small-to-medium sized molecules into monolayers is a means by which complex and functional nanostructures can be formed by a bottom-up strategy. Most multicomponent biological arrays form from the individual components by stepwise self-assembly processes and it is logical to use programmed self-organization processes for nanotechnology applications. Since the invention of scanning tunnelling microscopy (STM) and related scanning probe microscopic techniques, molecular-level studies of self-organized molecules on surfaces have increased dramatically. As a real-space and often real-time method, STM can give insights into the detailed molecular and supramolecular structures of such monolayers at a level that was previously inaccessible.[1–6] High-resolution images can be used to investigate single molecules or single molecule defects, dynamic processes and even the conformations of flexible adsorbed molecules. We are currently interested in the application of STM methods as a routine tool for solving structural problems of chemical relevance.[7–10]

Detailed predictions concerning the packing of molecules in a three-dimensional crystal lattice are generally not possible—indeed it is still one of the major challenges facing chemistry and physics in the 21st Century.[11] Prediction of packing will be influenced by the stoichiometry of the crystal (presence of solvent or other guest molecules) and by the possibility of polymorphism. It is marginally easier to make predictions about molecular assemblies in two dimensions, where the number of plane groups is only 17 compared to the 230 three-dimensional space groups.[12] Combining three-dimensional, single-crystal structural studies with investigations of two-dimensional monolayers of the same compounds might provide further clues to aid in the understanding of self-assembly and self-organization processes and may allow the prediction of monolayer structure and the designed construction of nanodevices from a knowledge of the bulk three-dimensional crystal structure or molecular structure.[13–16] The observation of two-dimensional layers in three-dimensional crystals is common[17] and studies of epitaxial thin films on graphite have established a correlation between two- and three-dimensional structure.[18–21]

In the growth of monolayers on atomically flat substrates, molecule–surface interactions are often strong enough to enforce a near-planar conformation on the adsorbate, even if the mean solution or gas-phase conformation of the molecule is non-planar. Aromatic ligands such as the oligopyridines might be expected to interact in a coplanar face-to-face manner with atomically flat substrates but only a few STM studies of flat-lying bpy,[7,8,22–26] phen[24,27] or tpy[7,8,28–31] derivatives on highly oriented pyrolytic graphite (HOPG) are known. In the case of the parent ligands bpy,[24,32–39] phen[40–45] and tpy[46] on d-block metal surfaces, the preferred conformation appears to be tilted or orthogonal to the substrate plane although the conformation is reported to be dependent upon the potental between the tip and the substrate, co-adsorbants or protonation. The latter observations are usually interpreted in terms of quasi-coordination interactions with the surface metal sites.

[a] *Department of Chemistry, University of Basel, Spitalstrasse 51, 4056 Basel, Switzerland. E-mail: edwin.constable@unibas.ch; Fax: +41 61 267 1005; Tel: +41 61 267 1001*
[b] *Institute of Physics, University of Basel, Klingelbergstrasse 82, 4056 Basel, Switzerland*

† The HTML version of this article has been enhanced with additional colour images.

‡ Present address: Tokyo Institute of Technology, Department of Biomolecular Engineering, 4259 Nagatsuta-cho, Midori-ku, Yokohama 226-8501, Japan.

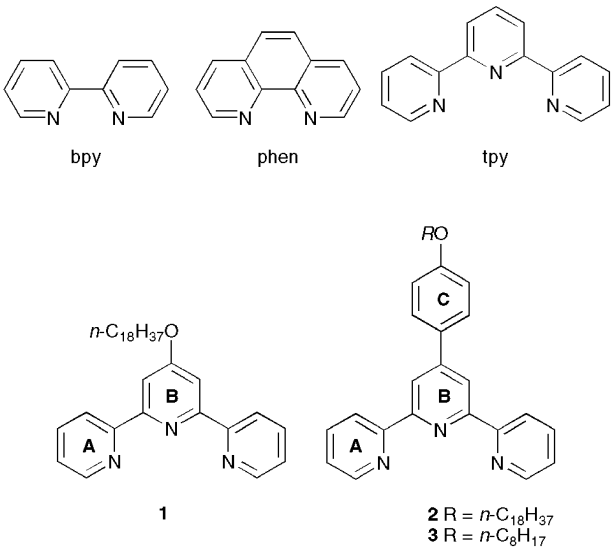

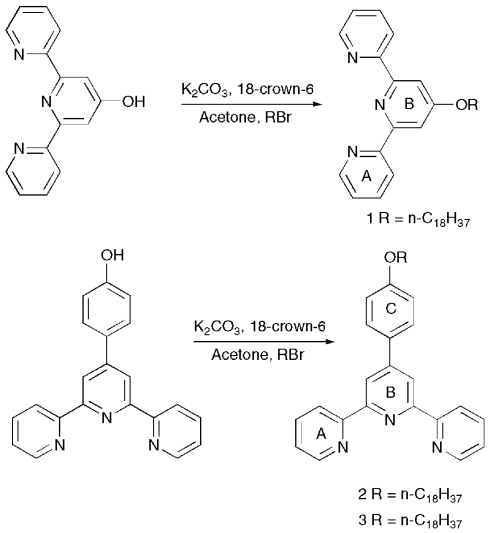

Scheme 1 Synthesis of ligands **1**, **2** and **3**.

In this paper, we present the synthesis, structural characterisation and STM studies of two tpy derivatives containing pendant octadecyl tails (**1** and **2**) that self-assemble on an HOPG surface. Each molecule in the monolayer possesses a free tpy coordination domain which has potential for further metal-mediated molecular assembly.[22] We also report preliminary results on the assembly of ligand **3** containing an octyl chain.

Results and discussion

Synthesis and structural characterisation of ligands 1, 2 and 3

Two methods are commonly utilised for the synthesis of 2,2′:6′,2″-terpyridinyl ethers; in the first, electrophilic 4′-chloro-2,2′:6′,2″-terpyridine is reacted with an alkoxide[28,47–53] and in the second, 4′-hydroxy-2,2′:6′,2″-terpyridine **4** is reacted with a haloalkane or related electrophile.[47–54] Only the latter strategy is applicable in the case of **2** and **3** which are derived from 4′-(4-hydroxyphenyl)-2,2′:6′,2″-terpyridine[55–57] **5**. Either **4** or **5** were treated with K_2CO_3 in the presence of 18-crown-6 to generate the corresponding phenoxide followed by addition of 1-bromooctadecane or 1-bromooctane and eventual chromatographic workup to give **1**, **2** and **3** in 85, 75 and 67% yields, respectively (Scheme 1). Compound **1** has previously been prepared from the reaction of 4′-chloro-2,2′:6′,2″-terpyridine with 1-octadecanol.[28] ^{1}H NMR spectra in $CDCl_3$ of compounds **1** and **2** were indicative of partially protonated species arising from the chromatographic work up. This was suppressed by the addition of a small amount of solid K_2CO_3. Well-resolved spectra were obtained by using a 1 : 1 mixture of $CDCl_3$ and CD_3OD. The pattern of ^{1}H NMR signals for protons H^{A6}, H^{A5}, H^{A4} and H^{A3} (see Scheme 1 for atom labelling) is similar for each of compounds **1**, **2** and **3**, while the signal for H^{B3} shifts to higher frequency on going from **1** (δ 7.87 ppm) to **2** (δ 8.53 ppm) or **3** (δ 8.74 ppm) when the aryl spacer is introduced. This is typical of other 4′-aryl tpy ligands and fully in accord with the expected deshielding effect of the phenyl ring.

X-Ray quality crystals of each of **1**, **2** and **3** were grown from hexane solutions. The molecular structure of **1** is shown in Fig. 1 and selected bond distances and angles are given in the figure caption. The three pyridine rings adopt the expected *trans*, *trans* conformation. The angles between the least squares planes of pyridine rings containing N1 and N2 and N2 and N3 are 7.78(8) and 9.13(8)°, respectively. The C(8)–O(1)–C(16) angle of 118.4(1)°, O(1)–C(8) bond distance of 1.360(2) Å (compare O(1)–C(16) 1.446(2) Å) and the torsion angle C(16–O(1)–C(8)–C(7) of 2.7(2)° are consistent with the expected sp^2 hybridization of the O atom and a degree of π-conjugation between the O atom and the central pyridine ring. The C_{18}-chain is in an extended conformation. Bond lengths and angles within the molecule closely resemble those in other structurally characterised alkoxy 2,2′:6′,2″-terpyridines.[28,58–64] The packing of the molecules in the solid state is interesting and contrasts with those of **2** and **3** described later. The structure contains domains of stacked molecules,

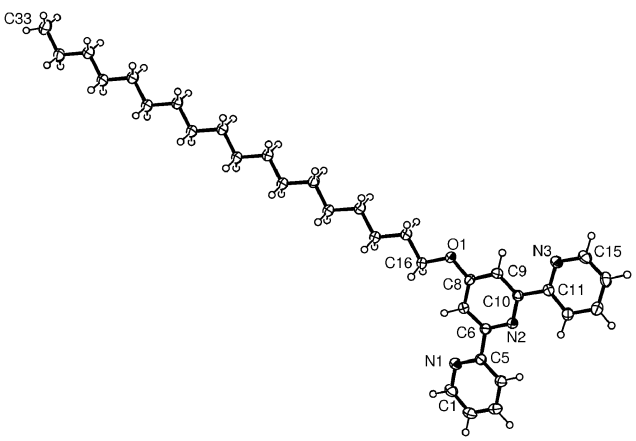

Fig. 1 Molecular structure of **1**. Selected bond distances (Å) and angles (°): O(1)–C(8) 1.360(2), O(1)–C(16) 1.446(2), N(1)–C(1) 1.339(2), N(1)–C(5) 1.348(2), N(2)–C(6) 1.342(2), N(2)–C(10) 1.348(2), N(3)–C(11) 1.345(2), N(3)–C(15) 1.344(2), C(5)–C(6) 1.495(2), C(10)–C(11) 1.491(2); C(8)–O(1)–C(16) 118.4(1), C(1)–N(1)–C(5) 116.9(2), C(6)–N(2)–C(10) 117.6(1), C(11)–N(3)–C(15) 116.6(1); torsion angle C(16)-O(1)-C(8)-C(7) 2.7(2)°.

aligned with the tpy units co-parallel, but offset with respect to one another, the closest atom (C···N) separation between adjacent molecules being 4.0 Å. Intermolecular interactions within the stacks are dominated by van der Waals interactions between adjacent alkyl chains (C···C 4.1 Å). The domains of stacked molecules are interdigitated, forming head-to-tail pairs. These paired domains are then arranged so that adjacent paired stacks are close to orthogonal (angle between least squares planes = 84.5°), resulting in the network illustrated in Fig. 2(a). When viewed along the *a*-axis, the domains of stacked molecules form a zigzag array (Fig. 2(b)).

The molecular structure of compound **2** is shown in Fig. 3 and selected bond parameters are listed in the caption. The three pyridine rings are deviate slightly from coplanarity (angles between the least squares planes of pyridine rings containing N1 and N2 and N2 and N3 are 10.72(7) and 9.25(7)°, respectively) and the central pyridine ring is coplanar with the aryl ring (angle between the least squares planes = 3.46(7)°). Structural parameters (see caption to Fig. 3) are consistent with the O atom being sp^2 hybridized and π-conjugation between the O atom and aryl spacer ring. The C_{18}-chain is again in an extended conformation. In the crystal lattice, molecules of **2** pack head-to-tail forming layers as shown in Fig. 4(a). This packing is presumably controlled by van der Waals interactions between the octadecyl chains.

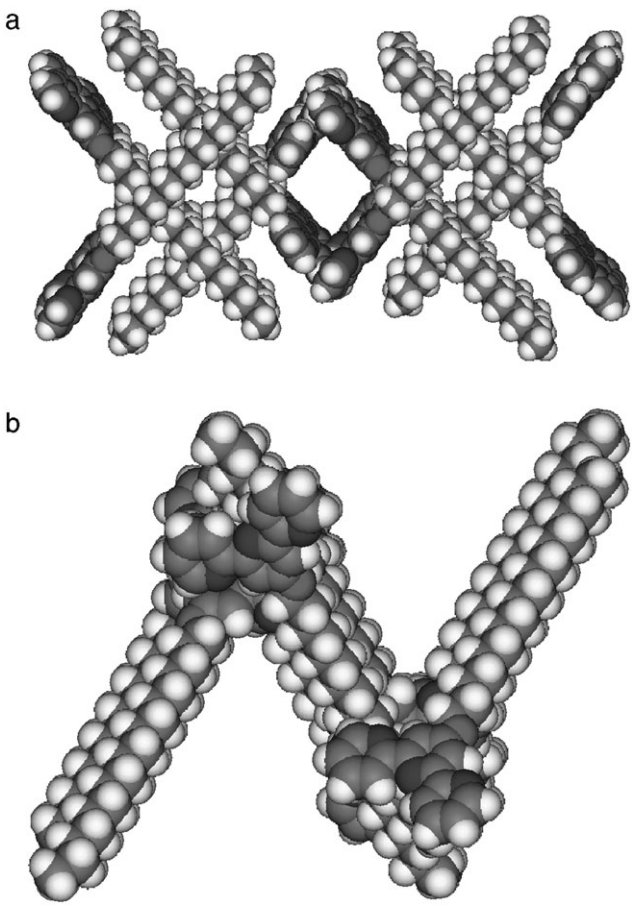

Fig. 2 Packing of molecules of **1** (a) viewed down the *c*-axis of two unit cells and (b) viewed down the *a*-axis.

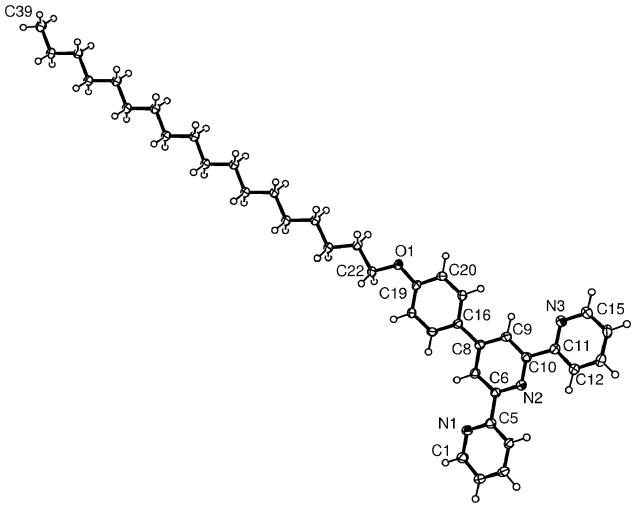

Fig. 3 Molecular structure of **2**. Selected bond distances (Å) and angles (°): O(1)–C(19) 1.372(2), O(1)–C(22) 1.439(2), N(1)–C(1) 1.337(2), N(1)–C(5) 1.349(2), N(2)–C(6) 1.346(2), N(2)–C(10) 1.345(2), N(3)–C(11) 1.345(2), N(3)–C(15) 1.337(2), C(5)–C(6) 1.484(2), C(10)–C(11) 1.491(2), C(8)–C(16) 1.490(2); C(19)–O(1)–C(22) 119.6(1), C(1)–N(1)–C(5) 117.3(1), C(6)–N(2)–C(10) 116.9(1), C(11)–N(3)–C(15) 117.4(1); torsion angle C(22)–O(1)–C(19)–C20 0.7(2)°.

Molecules are further assembled in stacks in which the C_6H_4–tpy units are π-stacked. The least squares planes containing the aryl and central pyridine ring of adjacent molecules deviate from coplanarity by 3.1° and the closest contacts between the plane containing the aryl ring and atoms in the central pyridine ring lie in the range 3.36–3.49 Å.

The molecular structure of compound **3** is shown in Fig. 5 and selected bond parameters are given in the figure caption. As in **2**, the three pyridine rings are close to coplanar (angles between the least squares planes of pyridine rings containing N1 and N2 and N2 and N3 are 8.06(8) and 10.87(8)°, respectively)) and the central pyridine ring is coplanar with the aryl ring (angle between the least squares planes = 3.27(7)°). The octyl chain is in an extended conformation. Molecules of **3** pack in layers (Fig. 6(a)) in which there is interdigitation of octyl chains and well-defined domains of head-to-head tpy units. This mode of assembly mimics that in **2**, as does the stacking of molecules (Fig. 6(b)). The least squares planes containing the aryl and central pyridine ring of adjacent molecules in the stacks deviate from coplanarity by 2.9°; the closest contacts between the plane containing the aryl ring and atoms in the central pyridine ring are in the range 3.35–3.51 Å.

Self-assembly on a graphite surface

Monolayers of compounds **1**, **2** and **3** were prepared on HOPG and investigated using STM. Monolayers of compound **1** have previously been studied by STM methods,[28] providing an independent confirmation for our results and interpretation. These observations usefully confirm the reproducibility of self-organisation processes in different laboratories using different techniques for the preparation of the monolayers. Since molecules containing long alkyl chains

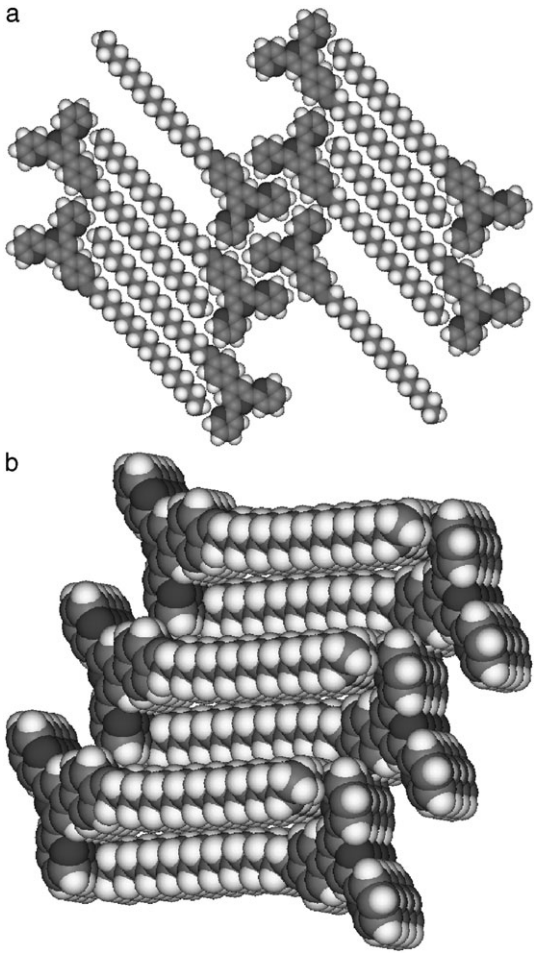

Fig. 4 (a) Part of a layer of molecules in the three-dimensional structure of **2**. (b) Packing of molecules of **2** viewed down the *b*-axis.

often require a relatively long time for organized self-assembly, the commonly utilised solution casting method does not reproducibly yield organized layers, although annealing of samples at temperatures around 80 °C can produce organized regions on the surface. The use of slow-evaporating solvents,

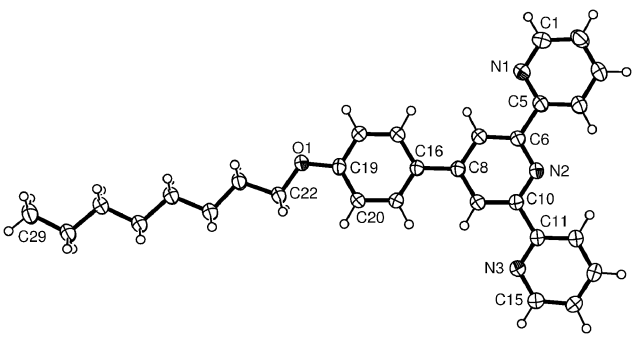

Fig. 5 Molecular structure of **3**. Selected bond distances (Å) and angles (°): O(1)–C(19) 1.367(2), O(1)–C(22) 1.433(2), N(1)–C(1) 1.338(2), N(1)–C(5) 1.343(2), N(2)–C(6) 1.341(2), N(2)–C(10) 1.345(2), N(3)–C(11) 1.345(2), N(3)–C(15) 1.336(2), C(8)–C(16) 1.481(2), C(5)–C(6) 1.489(2), C(10)–C(11) 1.484(2); C(19)–O(1)–C(22) 119.5(1), C(1)–N(1)–C(5) 117.4(1), C(6)–N(2)–C(10) 116.9(1), C(11)–N(3)–C(15) 117.6(1); torsion angle C(22)–O(1)–C(19)–C20 0.8(2)°.

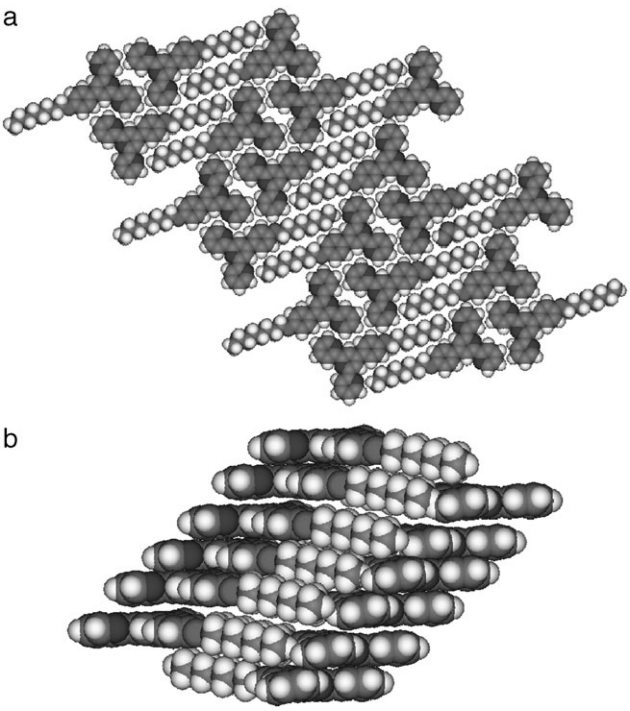

Fig. 6 Part of the packing diagram for compound **3** showing (a) interdigitation of the alkyl chains and assembly of molecules into layers and (b) π-stacking between aryl and central pyridine rings.

or measurements at the solid–liquid interface, allows molecules to pack in an optimal manner and attain a minimum energy two-dimensional structure. Most of the measurements reported in this study were made at the solid–liquid interface; a droplet of a near-saturated 1-phenyloctane solution of the ligand was placed on a freshly cleaved HOPG surface. STM measurements reveal that the molecules immediately form

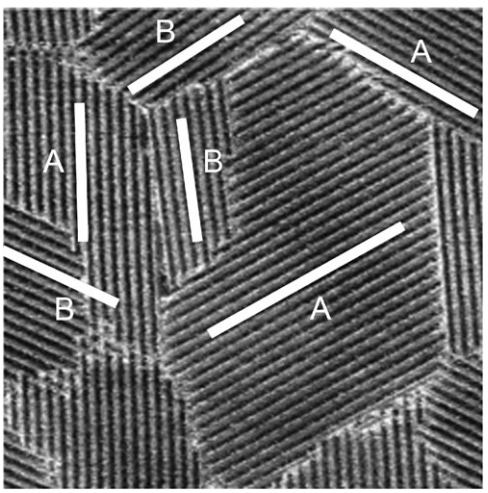

Fig. 7 (a) STM image of a monolayer of **1** at the 1-phenyloctane–graphite interface showing six domain orientations. Parameters: size 160 nm × 160 nm, U_{bias} = −700 mV, I_t = 15 pA. The A and B domains each possess the expected internal 120° and 240° relationships, but the angular relationship of individual A and B domains is ±4.4°, 120 ± 4.4° or 240 ± 4.4°.

lamellae composed of bright (aromatic) and dark (aliphatic) stripes, as expected for aromatic molecules functionalised with alkyl chains.

The STM images of monolayers of **1**, **2** and **3** consisted of striped patterns organized into domains with different orientations. Whereas a single graphite sheet has a six-fold symmetry, α-graphite possesses an effective threefold symmetry as a consequence of the ABAB layer structure in which every second atom in the A layer has an atom from the B layer directly underneath it and molecular assemblies on graphite are expected to have three equivalent orientations related to one another by angles of 120°.[65] However, for each of the three compounds, two subsets of domains each comprising three component orientations related by 120° with angular relationships 0, 120, 240, ±α, 120 ± α, 240 ± α were observed. Fig. 7 shows an STM measurement of **1**, with six different orientations of domains. In Fig. 7, the two sets of three domains are shown by the are indicated by the A and B labeled bars. The angle α between the sets of domains is 4.4° for **1**, 24.1° for **2** and 18.3° for **3**. The detailed origin of the domains is discussed later.

Detailed structural analysis

Reproducible high-resolution images allowed a detailed analysis of the molecular and supramolecular structure of the

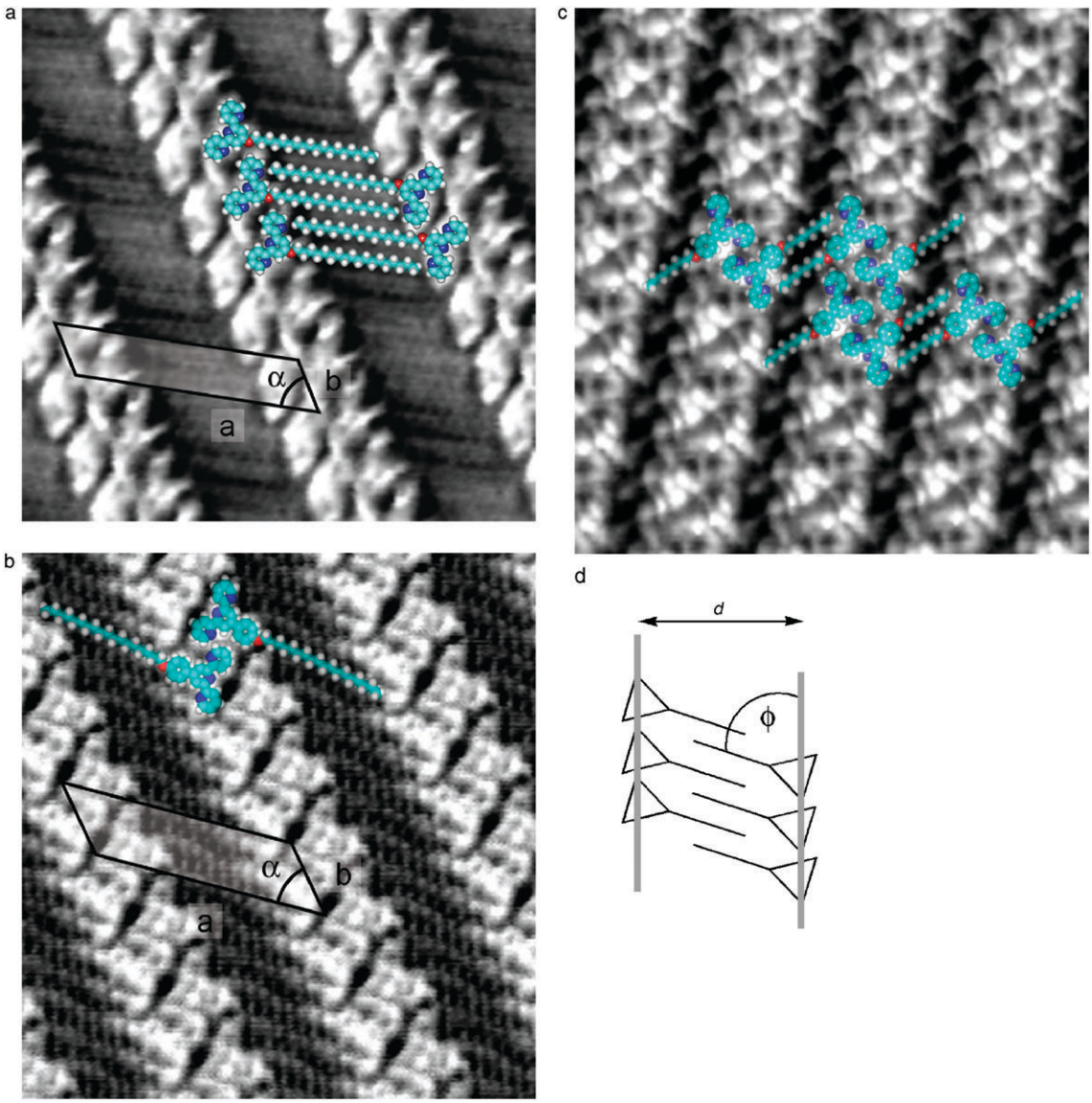

Fig. 8 Averaged STM images obtained at the solid–liquid interface of monolayers of (a) **1**, (b) **2** and (c) **3** under 1-phenyloctane with superimposed molecular structures and showing the unit cell in the cases of compounds **1** and **2**. The high-resolution images reveal that the alkanes have the carbon backbone parallel to the surface: (a) the layer of **1** is constructed by docking single molecules from the crystal structure constrained to two dimensions; in (b) and (c) the molecular structures are layers of molecules taken directly from the three-dimensional crystal structure. Parameters for (a), (b) and (c): 10 nm × 10 nm (all) (a) $U_{bias} = -700$ mV, $I_t = 20$ pA, averaged over 21 positions; (b) $U_{bias} = -440$ mV, $I_t = 20$ pA, averaged over 17 positions; (c) $U_{bias} = -550$ mV, $I_t = 14$ pA, averaged over 57 positions. Cartoon (d) shows the interlamellar spacing d and the angle ϕ between the alkyl chains and the direction of propagation of the aromatic stripes.

monolayers of **1**, **2** and **3** and a comparison with the three-dimensional structures obtained from single-crystal X-ray diffraction studies.[66] Averaging techniques allow high resolution STM images to be obtained.[67] For molecule **1**, our STM results are fully consistent with those reported by Schubert and co-workers.[28,30] In the monolayers of each compound, the alkyl chains are interdigitated and the terpyridine groups face each other, but are mutually offset. Fig. 8 shows averaged images of individual domains within monolayers of **1**, **2** and **3** with molecular structures overlaid. In the case of **2** and **3**, which both have sheets in the three-dimensional crystal structure, the overlaid structures are taken directly from the X-ray data and show that the two- and three-dimensional packing is the same for these compounds. In the case of **1**, where there is no sheet in the three-dimensional structure, a minimised array constrained to two dimensions with the observed periodicity is shown. In all cases, the match between the STM images and the molecular structures is excellent.

The interaction between an alkyl chain and the graphite surface increases regularly with the number of methylene groups[68–70] with a binding energy of 12–14.5 kJ mol^{-1} per CH_2 group and the strong interaction with the octadecyl chains results in highly-ordered monolayers giving particularly high-resolution STM images for compounds **1** and **2**. Alkanes lie flat on graphite surfaces with the C–C back-bone aligned with the C–C framework of the substrate.[71,72] The zigzag pattern of the alternating CH_2 groups of the alkyl chain lying flat on the graphite surface can easily be recognized in Fig. 8(a) and (b). Fig. 9 demonstrates unambiguously the orientation of the alkyl chains in an image in which the tunnelling current was switched from 10 pA in the top half of the scan, where the monolayer is imaged, to 100 pA in the bottom half, under which conditions the graphite is observed. The STM images for compound **3** (Fig. 8(c)) are less well-resolved, presumably as a consequence of the shorter C_8 chains not being adsorbed so strongly and retaining a degree of conformational freedom. A comparison of Fig. 8(a) and (b) is instructive. The periodicity is conveniently defined in terms of the spacing, *d*, between the conducting (light) lamellae, as measured by the orthogonal distance between the vectors of propagation (Fig. 8(d)). Intuitively, one expects the spacings in **2** which has an additional phenylene ring to be greater than in **1**. In practice the converse is true with orthogonal distances of 3.91 and 3.32 nm, respectively (in both domains). The high-resolution images reveal the origin of this phenomenon as the alkyl chains are directly imaged. These do not lie orthogonal to the direction of propagation of the stripes, but rather at an angle. The introduction of a single aryl spacer changes the pattern significantly. The alkyl chains for **2** are tilted more with respect to the striped pattern of the STM image than they are for **1** and this results in a much smaller periodicity of the stripes. The values are collected in Table 1.

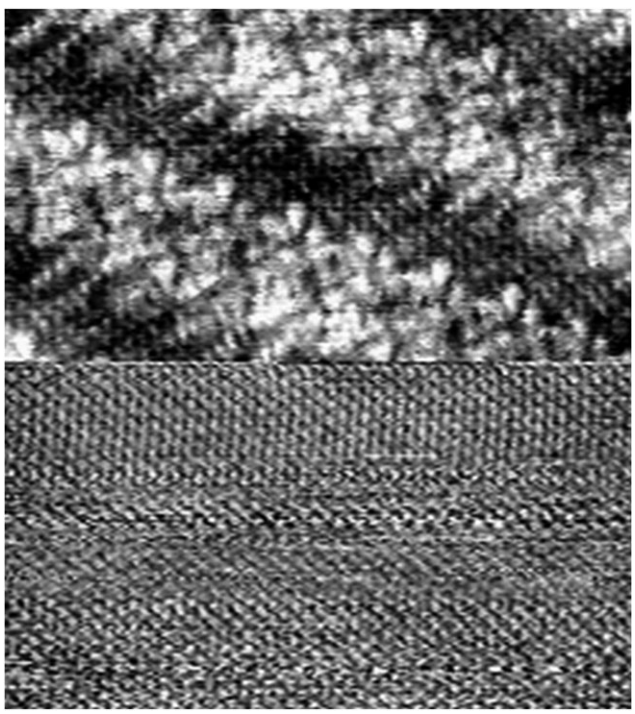

Fig. 9 STM image of **2**: $U_{bias} = -60$ mV and $I_t = 10$ pA in the top half of the scan and $I_t = 100$ pA in the bottom half showing the alignment of the alkyl chains with the graphite.

Table 1 Unit cell parameters and STM stripe-pattern periodicity for monolayers of **1**, **2** and **3**

Compound	Stripe periodicity /nm	*a*/nm	*b*/nm	*α*/°	Unit cell area/nm^2
1	3.91	4.5	1.1	60.3	4.2
2	3.32	4.3	1.4	50.4	4.6
3	2.54				

Symmetry breaking—from prochiral molecule to chiral adlayer

We have previously interpreted highly resolved STM images of multiple domains in monolayers of polyethers on HOPG in terms of differing conformations of the component molecules.[7–10] In the case of compounds **1–3** the origin is related but more general and will be discussed in detail for **2**. Consider molecule **2** constrained to a plane as in Fig. 10(a); two conformations are possible related by the orientation of the alkyl chain to the left or to the right. The two conformations

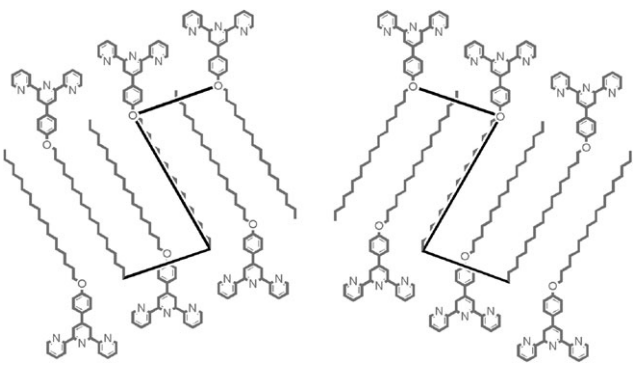

Fig. 10 (a) Compound **2** is prochiral with a left- or right-handed sense to the octadecyloxy substituent. (b) Adsorption of **2** on HOPG results in the formation of different patterns from the left- and right-handed molecules—the symmetry is broken and is conveniently represented by the vectors defining N and Ν shapes, respectively.

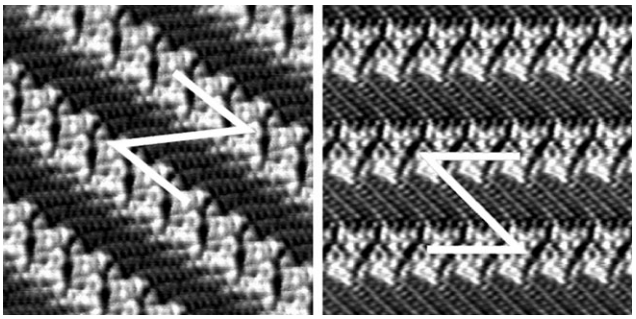

Fig. 11 Two averaged measurements of domains of compound **2** of different chirality at the air–solid interface. (a) A layer adsorbed on one face to form an N shape and (b) a layer adsorbed onto the other face, forming a ⋀⋁ shape. Parameters: size 10 nm × 10 nm (both). (a) $U_{bias} = -440$ mV, $I_t = 20$ pA, averaged over 20 positions in a single image. (b) $U_{bias} = -450$ mV, $I_t = 15$ pA, averaged over 21 positions in a single image.

are related as mirror images and compound **2** is correctly described as prochiral.

Under normal solution conditions, rotation about the C–O bond interconverts these two conformations, but adsorption onto a planar surface has two consequences; firstly, the interconversion of the two conformers becomes a high energy process and secondly, the definition of a face of the molecule converts **2** from being prochiral to chiral and the two conformers become enantiomers. We note that this phenomenon is intrinsically different from those observed in studies of monolayers of chiral molecules.[73] Although the symmetry-breaking consequences of adsorption have been commented on by a number of workers,[74–98] this phenomenon is still not widely appreciated in the chemical community. In this case, the interaction with the substrate results in a spectacular visual manifestation of the chirality. Fig. 9(b) shows the schematic arrangement of the two different enantiomers on a graphite surface, with the alkyl chain oriented along the C–C vectors of the substrate.[71,72] By adding lines corresponding to the alkyl chains and the principal direction of the aromatic domains, the two enantiomers are seen to describe N and ⋀⋁ patterns. Fig. 11 shows the same lines added to high-resolution STM images of different domains of **2** on HOPG and provides a visualisation of the symmetry-breaking and the formation of homochiral domains. We note that the results are analogous to, but strictly different from, studies on racemic chiral adsorbates.[98]

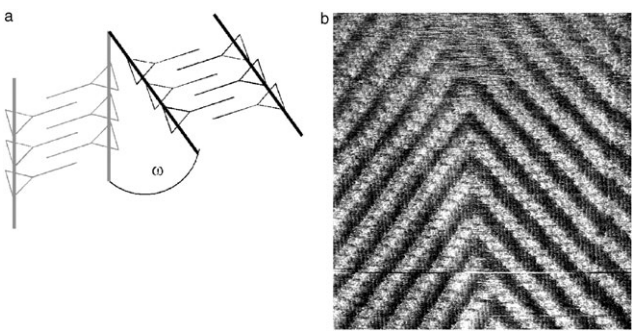

Fig. 12 (a) Representation of angular relationship between domains a domain boundary between two domains of differing chirality. The alkyl chains are oriented along a common graphite axis and with the stripes making the angle ω (24.1° in the case of **2**), which is related to the tilt angle between the alkyl chains and the aromatic stripes. (b) A relatively low resolution image at a domain boundary showing the common orientation of the alkyl chains in domains of different chirality.

The origin of the angular dependence of the domains is now clear. Individual domains are homochiral and domains with interdomain angles of 0°, 120° or 240° possess the same chirality. Domains with the $\pm\alpha^\circ$, $120 \pm \alpha^\circ$ or $240 \pm \alpha^\circ$ relationships are of opposite chirality. This is represented in Fig. 12. To summarise, the domains with the small angle relationships are homochiral and differ in their chirality as a result of the orientation of the left- and right-handed molecules on the substrate. Within domains of different chirality, all inter- and intramolecular interactions are the same—only the supramolecular interactions with the graphite substrate differ.

Conclusions

We have shown that three- and two-dimensional structural data may be correlated. For these tpy derivatives, if the three-dimensional crystal structure contains sheets, then these correspond to the structure of the two-dimensional monolayer on HOPG. If the three-dimensional crystal structure does not contain sheets, metrical data for individual molecules may be used to construct a two-dimensional array. It is interesting to speculate if three-dimensional polymorphs with the layer structures are possible in such cases.

Symmetry breaking results in the formation of homochiral domains when prochiral molecules are adsorbed onto a planar substrate.

Experimental

Infrared spectra were recorded on Mattson Genesis or Shimadzu FTIR 8300 Fourier-transform spectrophotometers with samples in compressed KBr discs or as solids using a Golden Gate ATR accessory. ^{1}H and ^{13}C NMR spectra were recorded on Bruker AM 250, AV 400 or DRX 500 spectrometers at room temperature; the numbering scheme adopted for the ligands is shown in Scheme 1 and chemical shifts are referenced with respect to internal TMS δ 0 ppm (for mixed solvents) or residual solvent peaks. EI mass spectra were recorded on a Kratos MS 50 instrument. Elemental analyses were carried out in the Department of Chemistry, University of Basel. Solvents were dried before use and reactions were carried out under N_2.

4′-(*n*-Octadecyloxy)-2,2′;6′,2″-terpyridine, 1

2,2′:6′,2″-Terpyridin-4′(1*H*)-one (500 mg, 2.00 mmol), K_2CO_3 (1.0 g, 7.2 mmol) and 18-crown-6 (0.21 g, 0.80 mmol) were added to acetone (20 ml) and the reaction mixture was heated at reflux for 30 min. 1-Bromooctadecane (669 mg, 2.00 mmol) was added to the mixture and was heated at reflux with stirring for 24 h. The crude product was obtained by filtering, washing with acetone and removing solvent *in vacuo*. After chromatography (Al_2O_3, eluted with CH_2Cl_2, 10% MeOH), **1** was

obtained as a white powder obtained (yield 0.85 g, 85%). White crystals suitable for X-ray diffraction were obtained by recrystallization with hexane. Melting point 95–97 °C (lit: 98–99 °C[11]). EI-MS m/z 501.5 $[M]^+$. ^{1}H NMR ($CDCl_3$–CD_3OH, 1 : 1, 250 MHz) δ/ppm 8.65 (m, H^{A6}, 2H), 8.48 (dt, J = 8.0, 1.2 Hz, H^{A3}, 2H), 7.96 (td, J = 7.7, 1.5 Hz, H^{A4}, 2H), 7.87 (s, H^{B3}, 2H), 7.45 (m, H^{A5}, 2H), 4.23 (t, CH_2, 2H, J = 6.3 Hz, OCH_2), 1.82 (m, CH_2, 2H, OCH_2CH_2), 1.45 (m, CH_2CH_3, 2H), 1.17 (m, CH_2, 28H), 0.79 (t, J = 6.8 Hz, CH_3, 3H); ^{13}C NMR ($CDCl_3$, 125 MHz) δ/ppm 168.0 (C^{B4}), 154.9, 154.4, 147.5, 138.9, 124.5, 122.5, 108.9, 69.2, 31.9, 29.7 (overlapping signals), 29.6 (overlapping signals), 29.4, 29.0, 26.0, 22.7, 14.1; IR (solid, cm^{-1}) $\bar{\nu}$ = 2916s, 2848s, 2360w, 2325w, 1281s, 1560s, 1469s, 1442s, 1402s, 1357m, 1278w, 1199s, 1143m, 1118m, 1095m, 1031s, 1024s, 989m, 916m, 881m, 867m, 794s, 746m, 732m, 717s, 700s, 659s, 646s. Calc. for $C_{33}H_{47}N_3O$: C, 79.00; H, 9.44; N, 8.37. Found: C, 78.78; H, 9.48; N, 8.19%.

4′-(4-*n*-Octadecyloxyphenyl)-2,2′:6′,2″-terpyridine, 2

4-(2,2′;6′,2″-Terpyridin-4′-yl)-phenol (500 mg, 1.54 mmol), K_2CO_3(1.0 g, 7.2 mmol) and 18-crown-6 (0.16 g, 0.61 mmol) were added to acetone (20 ml) and heated at reflux for 30 min. 1-Bromooctadecane (513 mg, 1.54 mmol) was added to the mixture and the reaction was heated at reflux with stirring for 24 h. Work-up was as for compound **1**. Compound **2** was obtained as a white powder (yield 670 mg, 75.4%). X-Ray quality crystals were obtained by recrystallization with hexane. Melting point 94 °C; EI-MS m/z 577.5 $[M]^+$; ^{1}H NMR ($CDCl_3$–CD_3OD 1 : 1, 250 MHz) δ/ppm 8.63 (m, H^{A6}, 2H), 8.57 (d, J = 8.0 Hz, H^{A3}, 2H), 8.53 (s, H^{B3}, 2H), 7.93 (td, 7.8, 1.8 Hz, H^{A4}, 2H), 7.81 (d(AB), J = 8.8 Hz, H^{C2}, 2H), 7.40 (m, H^{A5}, 2H), 6.99 (d(AB), J = 8.8 Hz, H^{C3}, 2H), 3.98 (t, J = 6.5 Hz, OCH_2, 2H), 1.75 (quintet, J = 7.0 Hz, OCH_2CH_2, CH_2, 2H), 1.42 (quintet, J = 7.0 Hz, CH_2CH_3, 2H), 1.18 (m, CH_2, 28H), 0.79 (t, J = 6.8 Hz, CH_3, 3H); ^{13}C NMR ($CDCl_3$–CD_3OD 1 : 1, 100 MHz) δ/ppm 159.9 (C^{C4}), 155.5, 155.0, 150.0, 148.2, 137.2, 129.5, 127.8, 123.7, 121.5, 117.8, 114.6 (C^{C3}), 67.7 (OCH_2), 31.4 ($CH_2CH_2CH_3$), 29.1 (overlapping signals), 29.0, 28.8, 28.7, 25.5, 22.1, 13.3 (CH_3); IR (solid, cm^{-1}) $\bar{\nu}$ = 2956m, 2931m, 2858m, 1598m, 1581s, 1564s, 1467m, 1442m, 1406m, 1350m, 1251w, 1201s, 1116w, 1091w, 999m, 979w, 871w, 794m, 734m, 659m, 622m. Calc. for $C_{39}H_{51}N_3O$: C, 81.06; H, 8.90; N, 7.27. Found: C, 80.94; H, 8.93; N, 7.23%.

4′-(4-*n*-Octyloxyphenyl)-2,2′:6′,2″-terpyridine, 3

4′-(4-Hydroxyphenyl)-2,2′:6′,2″-terpyridine (500 mg, 1.54 mmol), K_2CO_3 (1.0 g, 7.2 mmol) and 18-crown-6 (0.16 g, 0.61 mmol) were mixed in acetone (20 ml) and heated at reflux for 30 min. 1-Bromooctane (297 mg, 1.54 mmol) was added to the mixture and the reaction was heated at reflux with stirring for 24 h. Work-up was as for compound **1**. Compound **3** was obtained as a white powder (yield 450 mg, 67.2%). X-Ray quality crystals were obtained by recrystallization from hexane. Melting point 103 °C; EI-MS m/z 437.2 $[M]^+$; ^{1}H NMR ($CDCl_3$, 400 MHz) δ/ppm 8.744 (m, H^{A6}, 2H), 8.740 (s, H^{B3}, 2H), 8.69 (dt, J = 8.1, 1.2 Hz, H^{A3}, 2H), 7.90 (td, J = 7.7, 1.8 Hz, H^{A4}, 2H), 7.89 (d(AB), J = 9.0 Hz, H^{C2}, 2H), 7.37 (ddd, J = 7.5, 4.9, 1.2 Hz, H^{A5}, 2H), 7.02 (d(AB), J = 9.0 Hz, H^{C3}, 2H), 4.02 (t, J = 6.6 Hz, OCH_2 2H), 1.82 (quintet, J = 7.0 Hz, OCH_2CH_2, 2H), 1.48 (quintet, J = 7.0 Hz, CH_2CH_3, 2H), 1.30 (m, CH_2, 10H), 0.90 (t, J = 7.0 Hz, CH_3, 3H); ^{13}C NMR ($CDCl_3$, 100 MHz) 160.6 (C^{C4}), 156.4 ($C^{A2/B2}$), 155.7 ($C^{B2/A2}$), 150.4 (C^{B4}), 149.1 (C^{A6}), 137.8 (C^{A4}), 130.6 (C^{C1}), 128.9 (C^{C2}), 124.3 (C^{A3}), 122.0 (C^{A5}), 118.9 (C^{B3}), 115.3 (C^{C3}), 68.6 (OCH_2), 32.2($CH_2CH_2CH_3$), 29.8 (CH_2), 29.7 (CH_2), 29.6 (CH_2), 26.5 ($OCH_2CH_2CH_2$), 23.1 (CH_2CH_3), 14.5 (CH_3); IR (solid, cm^{-1}) 2914s, 2850s, 1600s, 1581s, 1566s, 1546s, 1515s 1467s, 1442s, 1421s, 1388s, 1361s, 1342m, 1317m, 1290m, 1257s, 1228s, 1186s, 1157s, 1128m, 1112s, 1074m, 1054s, 1037s, 1020m, 989s, 964m, 946m, 929m, 883s, 846s, 823s, 786s, 759s, 744s, 727s, 686m, 659s, 642m, 621m, 605m. Calc. for $C_{29}H_{31}N_3O$: C, 79.60; H, 7.14; N, 9.60. Found: C, 79.57; H, 7.18; N, 9.48%.

X-Ray crystallography

Determination of the cell parameters and collection of the reflection intensities were performed on an Enraf-Nonius Kappa CCD diffractometer (graphite-monochromated Mo-Kα radiation, λ = 0.710 73 Å. Structure determinations were by direct methods (Denzo/Scalepack,[99] SIR92[100]) and CRYSTALS[101] was used for structure refinement.

Compound 1. $C_{33}H_{47}N_3O$, M = 501.76, monoclinic, space group $C2/c$, a = 51.0346(8), b = 5.47280(10), c = 20.8564(3) Å, β = 95.9507(7)°, T = 173 K, V = 5793.85(16) Å^3, Z = 8, D_c = 1.150 g cm^{-3}, μ = 0.069 mm^{-1}, $F(000)$ = 2192. Number of reflections measured 13 763 (unique 6889); 3362 observed reflections ($I > 3\sigma(I)$); 335 parameters. The refinement converged at R = 0.0365, wR = 0.0459, max. and min. residual electron density 0.18 and −0.18 e Å^{-3}.

Compound 2. $C_{39}H_{51}N_3O$, M = 577.85, triclinic, space group $P\bar{1}$, a = 6.45410(10), b = 10.0694(2), c = 26.7131(6) Å, α = 98.7916(11), β = 93.2600(14), γ = 107.2415(13)°, T = 123 K, V = 1628.93(6) Å^3, Z = 2, D_c = 1.178 g cm^{-3}, μ = 0.070 mm^{-1}, $F(000)$ = 628. Number of reflections measured 15 143 (unique 7732); 3956 observed reflections ($I > 2\sigma(I)$); 389 parameters. The refinement converged at R = 0.0399, wR = 0.0360, max. and min. residual electron density 0.20 and –0.20 e Å^{-3}.

Compound 3. $C_{29}H_{31}N_3O$, M = 437.58, triclinic, space group $P\bar{1}$, a = 6.4461(3), b = 10.3457(5), c = 18.8455(8) Å, α = 83.808(3), β = 86.289(3), γ = 72.097(2)°, T = 173 K, V = 1188.30(10) Å^3, Z = 2, D_c = 1.223 g cm^{-3}, μ = 0.075 mm^{-1}, $F(000)$ = 468. Number of reflections measured 10656 (unique 5475); 3247 observed reflections ($I > 3\sigma(I)$); 298 parameters. The refinement converged at R = 0.0725, wR = 0.0965, max. and min. residual electron density 0.29 and –0.33 e Å^{-3}.

CCDC reference numbers 274895–274897.

For crystallographic data in CIF or other electronic format see DOI: 10.1039/b608136c

STM: general

A Nanoscope III, equipped with a low-current converter was used in all measurements. The tips were mechanically cut from Pt–Ir (90 : 10) wire. The piezo-scanner was carefully calibrated with Si-grids and HOPG atoms (for the *X*- and *Y*-axes) and with atomic gold steps (for the *Z*-axis). The apparent height in STM images is not a height of the molecule but a relative value which describes the relative conductivity/tunnelling of the molecules *vs*. the surrounding medium. All images presented in this paper were flattened, but no other image-manipulation or filtering was applied, with the exception of the averaging procedure (see figure captions). The measurements were repeated with different solutions on different substrate pieces with different STM tips. All measurements presented here were measured at the solution–graphite interface, with the exception of Fig. 11 for which the measurement was at a graphite-air interface.

STM: averaging procedure

The low tunnelling currents used in this study have the drawback of an increased noise level. This can be reduced by application of an averaging procedure. We used one programmed for the SXM-shell (©University of Basel);[8,9,67,102] a "sub-image" is cut from the original image and similar sub-images are then selected with help of a cross-correlation. After manual de-selection of faulted areas, the routine cuts sub-images at the selected places and an averaged image of all these is calculated. Great care was taken to compare the original with the averaged images, in order to exclude averaging artefacts.

Acknowledgements

We thank the Swiss National Science Foundation NRP 47 programme, the National Center of Competence in Research in Nanoscale Science and the University of Basel for financial support of this work. We thank Dr Lukas Scherer for many fruitful discussions.

References

1 G. Binnig and H. Rohrer, *Helv. Phys. Acta*, 1982, **55**, 726.
2 G. Binnig, H. Rohrer, C. Gerber and E. Weibel, *Phys. Rev. Lett.*, 1982, **49**, 57.
3 L. E. C. van de Leemput and H. van Kempen, *Rep. Prog. Phys.*, 1992, **55**, 1165.
4 W. Ho, *J. Chem. Phys.*, 2002, **117**, 11033.
5 W.-D. Schneider, *Surf. Sci.*, 2002, **514**, 74.
6 P. Samorí, *J. Mater. Chem.*, 2004, **14**, 1353.
7 E. C. Constable, B. A. Hermann, C. E. Housecroft, L. Merz and L. J. Scherer, *Chem. Commun.*, 2004, 928.
8 L. J. Scherer, L. Merz, C. E. Housecroft, E. C. Constable and B. A. Hermann, *J. Am. Chem. Soc.*, 2005, **127**, 4033.
9 L. Merz, L. H.-J. Güntherodt, L. J. Scherer, E. C. Constable, C. E. Housecroft, M. Neuburger and B. A. Hermann, *Chem. Eur. J.*, 2005, **11**, 2307.
10 B. A. Hermann, L. J. Scherer, C. E. Housecroft and E. C. Constable, *Adv. Funct. Mater.*, 2006, **16**, 221.
11 J. Maddox, *Nature (London)*, 1988, **335**, 201.
12 *International Tables for Crystallography*, ed. T. Hahn, Kluwer, Dordrecht, Netherlands, 4th edn, 1995, vol. A.
13 R. Azumi, G. Götz, T. De Baerdemaeker and P. Bäuerle, *Chem.-Eur. J.*, 2000, **6**, 735.
14 S. De Feyter, A. Gesquière, K. Wurst, D. B. Amabilino, J. Veciana and F. C. De Schryver, *Angew. Chem., Int. Ed.*, 2001, **40**, 3217.
15 E. Mena-Osteritz, *Adv. Mater.*, 2002, **14**, 609.
16 Z.-C. Mu, J.-F. Kong, Y. Wang, L. Ye, G.-D. Yang and X. Zhang, *ChemPhysChem*, 2004, **5**, 202.
17 G. Z. Mao, L. Lobo, L. R. Scaringe and M. D. Ward, *Chem. Mater.*, 1997, **9**, 773.
18 M. D. Ward, *Curr. Opin. Colloid Interface Sci.*, 1997, **2**, 51.
19 M. D. Ward, *Chem. Rev.*, 2001, **101**, 1697.
20 D. E. Hooks, T. Fritz and M. D. Ward, *Adv. Mater. (Weinheim. Ger.)*, 2001, **13**, 227.
21 J. A. Last, D. E. Hooks, A. C. Hillier and M. D. Ward, *J. Phys. Chem. B*, 1999, **103**, 6723.
22 S. De Feyter, M. M. S. Abdel-Mottaleb, N. Schuurmans, B. J. V. Verkuijl, J. H. Van Esch, B. L. Feringa and F. C. De Schryver, *Chem.-Eur. J.*, 2004, **10**, 1124.
23 L. Pan, J. Lu, Q. Zeng, S. Lei, Z. Tan, L. Wan and C. Bai, *Chin. Sci. Bull.*, 2003, **48**, 2450.
24 L. S. Pinheiro and M. L. A. Temperini, *Surf. Sci.*, 1999, **441**, 45.
25 M. M. S. Abdel-Mottaleb, N. Schuurmans, S. De Feyter, J. V. Esch, B. L. Feringa and F. C. De Schryver, *Chem. Commun.*, 2002, 1894.
26 B. Xu, S. Yin, C. Wang, Q. Zeng, X. Qiu and C. Bai, *Surf. Interface Anal.*, 2001, **32**, 245.
27 M. Sugimasa, J. Inukai and K. Itaya, *J. Electrochem. Soc.*, 2003, **150**, E266.
28 P. R. Andres, R. Lunkwitz, G. R. Pabst, K. Boehn, D. Wouters, S. Schmatloch and U. S. Schubert, *Eur. J. Org. Chem.*, 2003, **3769**.
29 C. Grave, D. Lentz, A. Schaefer, P. Samori, J. P. Rabe, P. Franke and A. D. Schlueter, *J. Am. Chem. Soc.*, 2003, **125**, 6907.
30 D. Wouters, S. Hoppener, R. Lunkwitz, L. F. Chi, H. Fuchs and U. S. Schubert, *Adv. Funct. Mater.*, 2003, **13**, 277.
31 S. Bernhard, K. Takada, D. J. Diaz, H. D. Abruña and H. Murner, *J. Am. Chem. Soc.*, 2001, **123**, 10265.
32 T. Dretschkow, D. Lampner and T. Wandlowski, *J. Electroanal. Chem.*, 1998, **458**, 121.
33 T. Dretschkow and T. Wandlowski, *Electrochim. Acta*, 1999, **45**, 731.
34 T. Dretschkow and T. Wandlowski, *Top. Appl. Phys.*, 2003, **85**, 259.
35 T. Dretschkow and T. Wandlowski, *J. Electroanal. Chem.*, 1999, **467**, 207.
36 C. Du, B. Xu, Y. Li, C. Wang, S. Wang, Z. Shi, H. Fang, S. Xiao and D. Zhu, *New J. Chem.*, 2001, **25**, 1191.
37 F. Cunha, N. J. Tao, X. W. Wang, Q. Jin, B. Duong and J. D'Agnese, *Langmuir*, 1996, **12**, 6410.
38 H. Noda, T. Minoha, L. J. Wan and M. Osawa, *J. Electroanal. Chem.*, 2000, **481**, 62.
39 L. S. Pinheiro and M. L. A. Temperini, *Appl. Surf. Sci.*, 2001, **171**, 89.
40 L. S. Pinheiro and M. L. A. Temperini, *Surf. Sci.*, 1999, **441**, 53.
41 K. H. Lee, Y. Suh, C. Lee, Y. G. Hwang, H. J. Koo and M. H. Whangbo, *J. Phys. Chem. B*, 2005, **109**, 15322.
42 F. Cunha, Q. Jin, N. J. Tao and C. Z. Li, *Surf. Sci.*, 1997, **389**, 19.
43 M. M. Gomez, M. P. Garcia, J. San Fabian, L. Vazquez, R. C. Salvarezza and A. J. Arvia, *Langmuir*, 1996, **12**, 818.
44 M. Sugimasa, J. Inukai and K. Itaya, *J. Electrochem. Soc.*, 2003, **150**, E266.
45 V. Kalsani, H. Ammon, F. Jackel, J. P. Rabe and M. Schmittel, *Chem.-Eur. J.*, 2004, **10**, 5481.
46 L. S. Pinheiro and M. L. A. Temperini, *Surf. Sci.*, 2000, **464**, 176.
47 H. S. Chow, E. C. Constable and C. E. Housecroft, *Dalton Trans.*, 2003, 4568.
48 H. S. Chow, E. C. Constable, C. E. Housecroft, M. Neuburger and S. Schaffner, *Polyhedron*, 2006, **25**, 1831.
49 H. S. Chow, E. C. Constable, C. E. Housecroft, M. Neuburger and S. Schaffner, *Dalton Trans.*, 2006, 2880.
50 C. B. Smith, E. C. Constable, C. E. Housecroft and B. M. Kariuki, *Chem. Commun.*, 2002, 2068.
51 E. C. Constable, C. E. Housecroft and C. B. Smith, *Inorg. Chem. Commun.*, 2003, **6**, 1011.
52 E. C. Constable, C. E. Housecroft, M. Neuburger and C. Smith, *Dalton Trans.*, 2005, 2259.

53 E. C. Constable, C. E. Housecroft, B. M. Kariuki and C. B. Smith, *Supramol. Chem.*, 2006, **18**, 305.
54 P. R. Andres, H. Hofmeier, B. G. G. Lohmeijer and U. S. Schubert, *Synthesis*, 2003, 2865.
55 W. Spahni and G. Calzaferri, *Helv. Chim. Acta*, 1984, **67**, 450.
56 N. Kalyanam, M. A. Likhate and S. G. Manjunatha, *Indian J. Chem., Sect. B*, 1992, **31**, 555.
57 M. Licini and J. A. G. Williams, *Chem. Commun.*, 1999, 1943.
58 R.-A. Fallahpour, M. Neuburger and M. Zehnder, *Polyhedron*, 1999, **18**, 2445.
59 R. Kroll, C. Eschbaumer, U. S. Schubert, M. R. Buchmeiser and K. Wurst, *Macromol. Chem. Phys.*, 2001, **202**, 645.
60 D. Armspach, E. C. Constable, C. E. Housecroft, M. Neuburger and M. Zehnder, *Supramol. Chem.*, 1996, **7**, 97.
61 D. Armspach, E. C. Constable, C. E. Housecroft, M. Neuburger and M. Zehnder, *J. Organomet. Chem.*, 1998, **550**, 193.
62 E. C. Constable, T. Kulke, M. Neuburger and M. Zehnder, *New J. Chem.*, 1997, **21**, 633.
63 E. C. Constable, C. E. Housecroft, M. Neuburger, S. Schaffner and L. J. Scherer, *Dalton Trans.*, 2004, 2635.
64 R. Hoogenboom, P. R. Andres, G. Kickelbick and U. S. Schubert, *Synlett*, 2004, 1779.
65 D. Tománek and S. G. Louie, *Phys. Rev. B: Condens. Matter*, 1988, **37**, 8327.
66 E. Plass Katherine, K. Kim and J. Matzger Adam, *J. Am. Chem. Soc.*, 2004, **126**, 9042–9053.
67 W. O. Saxton, T. J. Pitt and M. Horner, *Ultramicroscopy*, 1979, **4**, 343.
68 T. Müller, G. W. Flynn, A. T. Mathauser and A. V. Teplyakov, *Langmuir*, 2003, **19**, 2812.
69 K. R. Paserba and A. J. J. Gellman, *Chem. Phys.*, 2001, **115**, 6737.
70 K. R. Paserba and A. J. Gellman, *Phys. Rev. Lett.*, 2001, **86**, 4338.
71 Z. X. Xie, X. Xu, B. W. Mao and K. Tanaka, *Langmuir*, 2002, **18**, 3113.
72 J. P. Rabe and S. Buchholz, *Science*, 1991, **253**, 424.
73 D. M. Walba, F. Stevens, N. A. Clark and D. C. Parks, *Acc. Chem. Res.*, 1996, **29**, 591.
74 Z. Mu, Z. Wang, X. Zhang, K. Ye and Y. Wang, *J. Phys. Chem. B*, 2004, **108**, 19955.
75 M. Bohringer, R. Berndt and W. D. Schneider, *Chem. Unserer Zeit*, 2005, **39**, 326.
76 M. Bohringer, K. Morgenstern, W. D. Schneider and R. Berndt, *J. Phys.: Condens. Matter*, 1999, **11**, 9871.
77 M. Bohringer, K. Morgenstern, W. D. Schneider and R. Berndt, *Angew. Chem., Int. Ed.*, 1999, **38**, 821.
78 M. Bohringer, W. D. Schneider and R. Berndt, *Surf. Rev. Lett.*, 2000, **7**, 661.
79 M. Bohringer, W. D. Schneider and R. Berndt, *Angew. Chem., Int. Ed.*, 2000, **39**, 792.
80 S. De Feyter and F. C. De Schryver, *J. Phys. Chem. B*, 2005, **109**, 4290.
81 S. De Feyter, P. C. M. Grim, M. Rucker, P. Vanoppen, C. Meiners, M. Sieffert, S. Valiyaveettil, K. Mullen and F. C. De Schryver, *Angew. Chem., Int. Ed.*, 1998, **37**, 1223.
82 C. B. France and B. A. Parkinson, *J. Am. Chem. Soc.*, 2003, **125**, 12712.
83 A. Gesquiere, P. Jonkheijm, F. J. M. Hoeben, A. Schenning, S. De Feyter, F. C. De Schryver and E. W. Meijer, *Nano Lett.*, 2004, **4**, 1175.
84 B. I. Kim, C. Z. Cai, X. B. Deng and S. S. Perry, *Surf. Sci.*, 2003, **538**, 45.
85 C. J. Li, Q. D. Zeng, P. Wu, S. L. Xu, C. Wang, Y. H. Qiao, L. J. Wan and C. L. Bai, *J. Phys. Chem. B*, 2002, **106**, 13262.
86 R. Lim, J. Li, S. F. Y. Li, Z. Feng and S. Valiyaveettil, *Langmuir*, 2000, **16**, 7023.
87 G. P. Lopinski, D. J. Moffatt, D. D. Wayner and R. A. Wolkow, *Nature*, 1998, **392**, 909.
88 W. Mamdouh, H. Uji-i, A. Gesquiere, S. De Feyter, D. B. Amabilino, M. M. S. Abdel-Mottaleb, J. Veciana and F. C. De Schryver, *Langmuir*, 2004, **20**, 9628.
89 C. Meier, U. Ziener, K. Landfester and P. Weihrich, *J. Phys. Chem. B*, 2005, **109**, 21015.
90 A. Miura, P. Jonkheijm, S. De Feyter, A. Schenning, E. W. Meijer and F. C. De Schryver, *Small*, 2005, **1**, 131.
91 M. E. Stawasz and B. A. Parkinson, *Langmuir*, 2003, **19**, 10139.
92 Y. H. Wei, K. Kannappan, G. W. Flynn and M. B. Zimmt, *J. Am. Chem. Soc.*, 2004, **126**, 5318.
93 S. Weigelt, C. Busse, L. Petersen, E. Rauls, B. Hammer, K. V. Gothelf, F. Besenbacher and T. R. Linderoth, *Nat. Mater.*, 2006, **5**, 112.
94 P. Wu, Q. D. Zeng, S. D. Xu, C. Wang, S. X. Yin and C. L. Bai, *ChemPhysChem*, 2001, **2**, 750.
95 D. G. Yablon, L. C. Giancarlo and G. W. Flynn, *J. Phys. Chem. B*, 2000, **104**, 7627.
96 H. M. Zhang, Z. X. Xie, B. W. Mao and X. Xu, *Chem.-Eur. J.*, 2004, **10**, 1415.
97 J. Zhang, A. Gesquiere, M. Sieffert, M. Klapper, K. Mullen, F. C. De Schryver and S. De Feyter, *Nano Lett.*, 2005, **5**, 1395.
98 R. Fasel, M. Parschau and K.-H. Ernst, *Nature*, 2006, **439**, 449.
99 Z. Otwinowski and W. Minor, *Methods Enzymol.*, 1997, **276**, 307.
100 A. Altomare, G. Cascarano, G. Giacovazzo, A. Guagliardi, M. C. Burla, G. Polidori and M. Camalli, *J. Appl. Crystallogr.*, 1994, **27**, 435.
101 P. W. Betteridge, J. R. Carruthers, R. I. Cooper, K. Prout and D. J. Watkin, *J. Appl. Crystallogr.*, 2003, **36**, 1487.
102 D. Brodbeck, D. Buergler, R. Hofer and G. Tarrach, University of Basel, 1993–2004.